



Development of a coumarin-furan conjugate as Zn^{2+} ratiometric fluorescent probe in ethanol-water system



Chao-ruì Li^a, Si-liang Li^{a,b}, Zheng-yin Yang^{a,*}

^a College of Chemistry and Chemical Engineering, State Key Laboratory of Applied Organic Chemistry, Lanzhou University, Lanzhou 730000, PR China

^b School of Petrochemical Engineering, Lanzhou University of Technology, Lanzhou 730050, PR China

ARTICLE INFO

Article history:

Received 9 August 2016

Received in revised form 18 November 2016

Accepted 19 November 2016

Available online 28 November 2016

Keywords:

Coumarin

Ratiometric fluorescent probe

Zinc ion

Selectivity

Sensitivity

ABSTRACT

In this study, a novel coumarin-derived compound bearing the furan moiety called 7-diethylamino-3-formylcoumarin (2'-furan formyl) hydrazone (**1**) has been designed, synthesized and evaluated as a Zn^{2+} ratiometric fluorescent probe in ethanol-water system. This probe **1** showed good selectivity and high sensitivity towards Zn^{2+} over other metal ions investigated, and a decrease in fluorescence emission intensity at 511 nm accompanied by an enhancement in fluorescence emission intensity at 520 nm of this probe **1** was observed in the presence of Zn^{2+} in ethanol-water (V : V = 9 : 1) solution, which provided ratiometric fluorescence detection of Zn^{2+} . Additionally, the ratiometric fluorescence response of **1** to Zn^{2+} was nearly completed within 0.5 min, which suggested that this probe **1** could be utilized for sensing and monitoring Zn^{2+} in environmental and biological systems for real-time detection.

© 2016 Elsevier B.V. All rights reserved.

1. Introduction

As we all know, zinc is the second most abundant transition metal element in the human body with its concentrations ranging from nanomolar (nM) to millimolar (mM) [1], and it is one of the most important transition metals in living systems [2]. The research of zinc ion (Zn^{2+}) has drawn considerable interests among chemists, biologists, environmentalists and pharmacologists due to its chemical and physical properties [3–6]. Zn^{2+} plays a crucial role in various biological processes such as neurotransmission [7], DNA synthesis [8], gene transcription [9], apoptosis [10], enzyme catalysis [11], immune function [12], mammalian reproduction [13] and pathology [14]. It is well known that the average level of Zn^{2+} in adult human bodies is 2–3 g, and the intracellular concentration of Zn^{2+} is 10–100 mM [15–16]. Genetic abnormalities or environmental factors may lead to the disorder of Zn^{2+} metabolism in biological systems caused by the misregulation in the concentrations or activities of Zn^{2+} , which is associated with a variety of diseases like Alzheimer's disease [17], Parkinson's disease [18], epilepsy [19], cerebral ischemia [20], amyotrophic lateral sclerosis (ALS) [21], diabetes [22] and infantile diarrhea [23]. Therefore, it is highly desirable to develop a convenient and rapid method for detecting Zn^{2+} to maintain its concentration in a suitable level in biological systems [24].

Owing to the relevant advantages like good selectivity, high sensitivity, inexpensive apparatus, simple sample preparation, real-time

detection and non-destructive properties, fluorescence detection has attracted serious concerns of chemists, biologists, environmentalists and pharmacists [25–28]. In recent years, a number of fluorescent probes for detecting and recognizing Zn^{2+} have been studied by various groups [29–32], but some of them can be applied only in organic solutions, which restricts their potential applications in environmental and biological systems [33]. Additionally, some Zn^{2+} fluorescent probes display relatively low selectivity and suffer from the interferences from other metal ions, especially Cd^{2+} [34], which is the same group as Zn^{2+} in the periodic table and has similar spectroscopic properties with that of Zn^{2+} [35]. Therefore, when these two metal ions are coordinated with probe molecule respectively, the similar changes of fluorescence intensities as well as the shift of wavelengths can be usually obtained [36]. Thus, it is a great challenge to design and synthesize a fluorescent probe to sense and monitor Zn^{2+} with high selectivity and sensitivity in aqueous solutions [37].

Intensity-based fluorescent probes in which the fluorescence intensity at a certain wavelength is only one signal can be affected by other variables like probe molecule concentrations, micro-environmental conditions or differences in optical components between instruments [38]. Comparably, ratiometric detection can overcome the limitations of those intensity-based fluorescent probes by measuring the ratio of the fluorescence intensities at two different wavelengths via self-calibration processes, so that they can provide quantitative measurements for a specific analyte [39]. As a result, the development of ratiometric fluorescent probes has attracted broad interests among chemists and biologists for detecting and monitoring metal ions in environmental and biological systems [40–44].

* Corresponding author.

E-mail address: yangzy@zu.edu.cn (Z. Yang).

Coumarin and its derivatives have been extensively utilized as medicines, fluorescent dyes and fluorescent probes, due to their excellent optical properties such as high fluorescence quantum yield, large Stock's shift, good photostability and nontoxicity [45–47]. Taking all these into consideration, we have designed and synthesized a novel coumarin-derived fluorescent probe bearing the furan moiety called 7-Diethylamino-3-formylcoumarin (2'-furan formyl) hydrazone (**1**) (Scheme 1), which showed ratiometric fluorescence response to Zn^{2+} in ethanol-water ($V : V = 9 : 1$) solution. A decrease in fluorescence emission intensity at 511 nm accompanied by an enhancement in fluorescence emission intensity at 520 nm of this probe **1** was observed in the presence of Zn^{2+} , which provided ratiometric fluorescence detection of Zn^{2+} , and **1** showed good selectivity and high sensitivity towards Zn^{2+} over other common metal ions, especially Cd^{2+} . Furthermore, the reversibility and regeneration of **1** were perfect and the ratiometric fluorescence response of **1** to Zn^{2+} was fast. Hence, owing to the good selectivity, high sensitivity and perfect reversibility for detecting and recognizing Zn^{2+} , this probe **1** could be utilized as a Zn^{2+} ratiometric fluorescent probe in environmental and biological systems for real-time detection.

2. Experimental

2.1. Materials

2-Furan formic acid, hydrogen peroxide, concentrated sulfuric acid, hydrazine hydrate, 4-diethylaminosalicylaldehyde, diethyl malonate, piperidine, hydrochloric acid, glacial acetic acid, sodium hydroxide, phosphorus oxychloride, absolute ethanol, *N,N*-dimethyl formamide (DMF), dimethyl sulfoxide (DMSO) and cationic salts such as $Zn(NO_3)_2$, $Al(NO_3)_3$, $Ba(OAc)_2$, $Ca(NO_3)_2$, $Cd(OAc)_2$, $Co(OAc)_2$,

$Cr(NO_3)_3$, $Cu(NO_3)_2$, $Fe(NO_3)_2$, $Fe(NO_3)_3$, $K(OAc)$, $Mg(NO_3)_2$, $Mn(NO_3)_2$, $NaClO_4$, $Ni(NO_3)_2$ and $Pb(OAc)_2$ were obtained from commercial suppliers, and used as received without further purification. Stock solution of compound **1** (10 mM) in DMSO was prepared, and stock solutions (10 mM) of the cationic salts of Zn^{2+} , Al^{3+} , Ba^{2+} , Ca^{2+} , Cd^{2+} , Co^{2+} , Cr^{3+} , Cu^{2+} , Fe^{2+} , Fe^{3+} , K^+ , Mg^{2+} , Mn^{2+} , Na^+ , Ni^{2+} and Pb^{2+} were also prepared in absolute ethanol. Distilled water was used throughout all experiments.

2.2. Apparatus

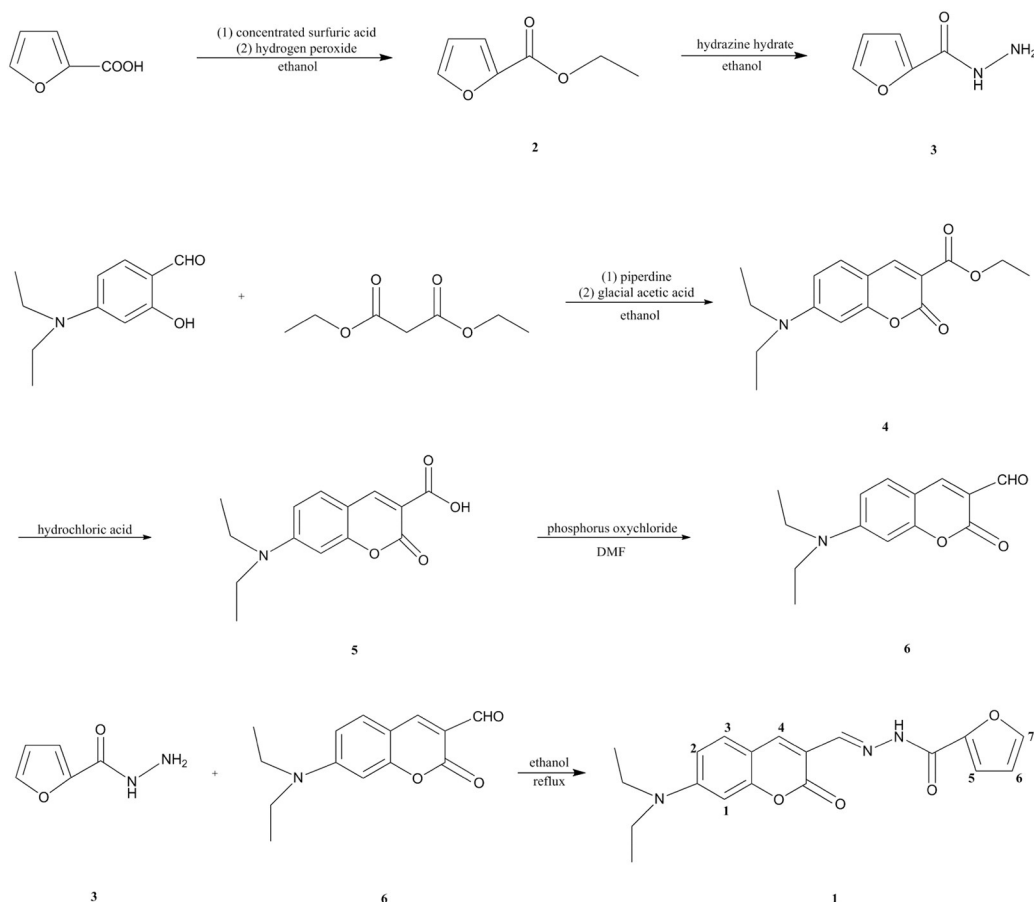
1H NMR spectra were measured on the JNM-ECS 400 MHz instruments spectrometers in $CDCl_3$ using TMS (tetramethylsilane) as an internal standard. The ESI-MS data were obtained in ethanol from a Bruke Esquire 6000 spectrometer. UV-vis absorption spectra were determined on a Shimadzu UV-240 spectrophotometer at 298 K. Fluorescence spectra were recorded on a Hitachi RF-5301 spectrophotometer equipped with quartz cuvettes of 1 cm path length at 298 K. Melting points were determined on a Beijing XT4-100x microscopic melting point apparatus without correction.

2.3. Synthesis

Ethyl 2-furan formate (**2**) and 2-furan formylhydrazine (**3**) were synthesized according to the reported method [48]. The synthetic route of compound **1** was shown in Scheme 1.

Synthesis of compound 1 (7-Diethylamino-3-formylcoumarin (2'-furan formyl) hydrazone).

Ethyl 7-diethylaminocoumarin-3-formate (**4**), 7-diethylaminocoumarin-3-formic acid (**5**) and 7-diethylamino-3-formylcoumarin (**6**) were prepared according to the method reported



Scheme 1. The synthetic route of compound **1**.

previously [49]. A solution of 2-furan formylhydrazine (**3**) (0.126 g, 1.000 mmol) in absolute ethanol (10 mL) was added dropwise to another solution containing 7-diethylamino-3-formylcoumarin (**6**) (0.245 g, 1.000 mmol) in absolute ethanol (30 mL) under stirring. The reaction mixture was stirred vigorously at room temperature for 12 h, during which time the color of the solution turned from orange yellow to orange red. Then half of the ethanol was evaporated under reduced pressure and the rest of solution was cooled to room temperature. After placing the solution into refrigerator for 4 h, an orange red solid was separated out from the solution and filtered under reduced pressure, washing five times with ice-cold ethanol (10 mL). The obtained crude product was recrystallized from absolute ethanol (30 mL) to furnish the desired product **1** as an orange yellow powder (Scheme 1). Yield: 0.11 g (31.16%). m.p. 239–242 °C, $^1\text{H NMR}$ (400 MHz, CDCl_3) (Fig. S1): 8.66 (s, 1H, —NH—), 7.80 (s, 1H, H_4), 7.69 (s, 1H, H_7), 7.02 (s, 1H, H_5), 6.91 (d, 1H, $J = 7.2$ Hz, H_3), 6.88 (s, 1H, H_6), 6.31 (dd, 1H, $J = 7.2$ Hz, $J = 1.6$ Hz, H_2), 6.26 (dd, 1H, $J = 2.8$ Hz, $J = 1.2$ Hz, —CH=N—), 6.20 (d, 1H, $J = 1.6$ Hz, H_1), 3.76 (q, 4H, $J = 5.6$ Hz, — CH_2 —), 1.99 (t, 6H, $J = 5.6$ Hz, — CH_3). MS (ESI) (Fig. S2): m/z [$\text{M} + \text{H}^+$] $^+$ calcd 354.3599, found 354.1438; [$\text{M} + \text{Na}^+$] $^+$ calcd 376.3418, found 376.1244; [$\text{M} + \text{K}^+$] $^+$ calcd 392.4503, found 392.0950; [$2\text{M} + \text{Na}^+$] $^+$ calcd 729.6937, found 729.2406. Anal. Calcd. for $\text{C}_{19}\text{H}_{19}\text{N}_3\text{O}_4$ (%): C, 64.58; H, 5.42; N, 11.89; O, 18.11. found: C, 65.24; H, 4.84; N, 8.84; O, 21.08.

2.4. General Information

Test solutions were prepared by placing 10 μL of the probe stock solution into cuvettes, adding an appropriate aliquot of each metal ion stock, and diluting the solution to 2 mL with ethanol-water ($V : V = 9 : 1$) solution. For all fluorescence measurements of compound **1**, the excitation wavelength was set at 322 nm and the fluorescence emission spectra were recorded over the range of 470–640 nm. The excitation and emission slit widths were 3 nm and 1.5 nm in fluorescence emission spectra of **1**, respectively.

The binding constant value for complex **1**- Zn^{2+} was determined on the basis of the nonlinear fitting of the fluorescence titration curve assuming a 2 : 1 stoichiometry by the Benesi–Hildebrand method [1] [50–51]:

$$\frac{1}{F - F_{\min}} = \frac{1}{K(F_{\max} - F_{\min})[\text{Zn}^{2+}]^{0.5}} + \frac{1}{(F_{\max} - F_{\min})} \quad (1)$$

where F_{\min} , F , and F_{\max} are the emission intensities at 520 nm of the organic moiety considered in the absence of zinc ion, at an intermediate zinc concentration, and at a concentration of complete interaction, respectively, and where K is the binding constant.

The limit of detection (LOD) of compound **1** for detecting Zn^{2+} was calculated from the fluorescence titration. The ratio of emission intensities at 520 nm and 511 nm ($F_{520 \text{ nm}}/F_{511 \text{ nm}}$) of compound **1** without any anion was measured to determine the S/N ratios [52–53], and the standard deviation of blank measurements was calculated. The LOD value was calculated based on $3 \times \sigma_{\text{blank}}/k$, where σ_{blank} is the standard deviation of the blank solution and k is the slope of the calibration plot.

3. Results and Discussion

3.1. Synthesis and Characterization of Compound **1**

Compound **1** was synthesized according to the synthetic route outlined in Scheme 1. Ethyl 2-furan formate (**2**) and 2-furan formylhydrazine (**3**) were synthesized according to the reported method [48]. Firstly, ethyl 7-diethylaminocoumarin-3-formate (**4**) was prepared by reacting 4-diethylaminosalicylaldehyde with diethyl malonate using piperidine and glacial acetic acid as catalysts under

refluxing in absolute ethanol. Then ethyl 7-diethylaminocoumarin-3-formate (**4**) was acidated in absolute ethanol to give **5** (7-diethylaminocoumarin-3-formic acid). Subsequently, **5** was reacted with phosphorus oxychloride in *N,N*-dimethyl formamide (DMF) and 7-diethylamino-3-formylcoumarin (**6**) was obtained. Finally, the condensation reaction between 2-furan formylhydrazine (**3**) and 7-diethylamino-3-formylcoumarin (**6**) in absolute ethanol furnished the desired compound **1** as an orange yellow powder. The structure of compound **1** was characterized by $^1\text{H NMR}$ and mass spectrometry (ESI-MS), and the details of the characterization data of compound **1** were presented in the Supporting Information (Fig. S1–S2).

3.2. UV-vis Titration of Compound **1** with Increasing Amounts of Zn^{2+}

In order to clarify the interaction of compound **1** with metal ions, the spectroscopic properties of **1** towards various chemically and biologically important metal ions were investigated by UV-vis and fluorescence methods in ethanol-water ($V : V = 9 : 1$) solution. In order to gain insight into the UV-vis response of compound **1** to Zn^{2+} , we firstly conducted the UV-vis absorption titration spectrum of compound **1** in the presence of increasing amounts of Zn^{2+} in ethanol-water ($V : V = 9 : 1$) solution and the results were shown in Fig. 1. There were almost no bands in the range from 230 nm to 600 nm in UV-vis absorption spectrum of free **1**, but two new bands centered at 342 nm and 474 nm appeared with increasing absorbance upon addition of various concentrations of Zn^{2+} (Fig. 1), which indicated that a new complex had been formed between compound **1** and Zn^{2+} in ethanol-water ($V : V = 9 : 1$) solution.

3.3. Fluorescence Titration of Compound **1** with Increasing Amounts of Zn^{2+}

The quantitative nature of compound **1** for sensing Zn^{2+} was then elucidated by conducting fluorescence emission spectrum of **1** in the presence of increasing amounts of Zn^{2+} in ethanol-water ($V : V = 9 : 1$) solution as described in Fig. 2. Upon excitation at 322 nm, compound **1** alone exhibited an intense emission peak centered at 511 nm. Wherever, with a continuous increase in Zn^{2+} concentration, a gradual decrease in emission intensity at 511 nm was observed. Simultaneously, a new emission peak centered at 520 nm appeared with increasing intensity and a well-defined isosomission point was obtained at 516 nm. It was probably because that the proton of hydrazone nitrogen atom

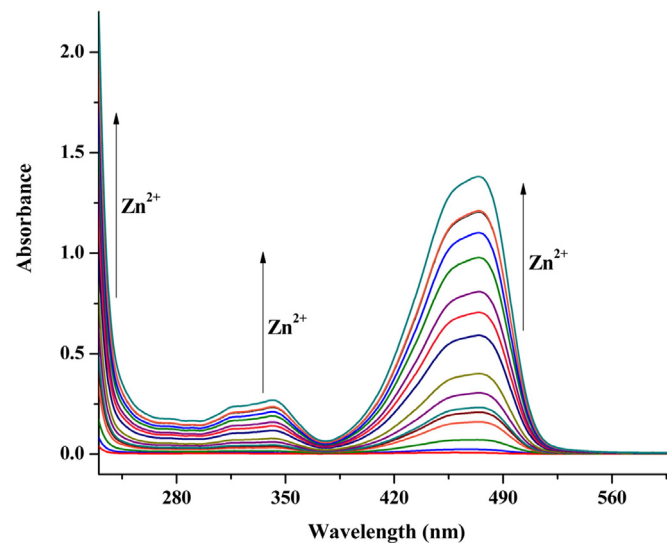


Fig. 1. Change in UV-vis absorption spectrum of **1** (100 μM) upon addition of increasing amounts of Zn^{2+} (0.2, 0.4, 0.6, 0.8, 1.0, 1.4, 1.8, 2.2, 2.6, 3.0, 3.4, 3.8, 4.2, 4.6, 5.0 equiv., respectively) in ethanol-water ($V : V = 9 : 1$) solution.

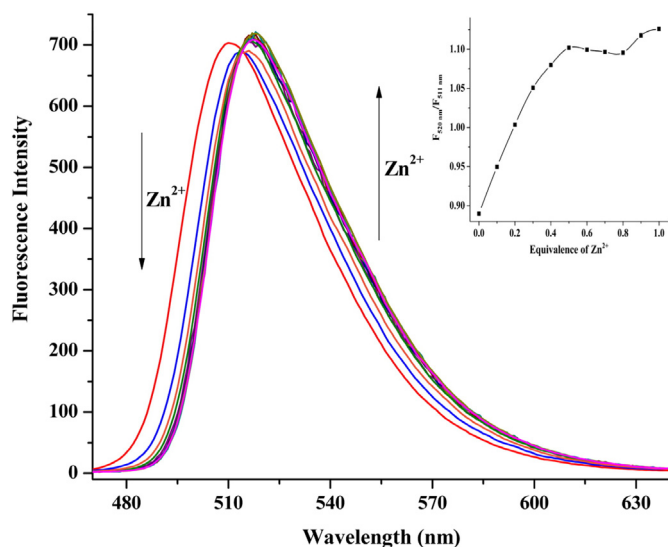


Fig. 2. Change in fluorescence emission spectrum of **1** (50 μM) upon addition of increasing amounts of Zn^{2+} (0.1, 0.2, 0.3, 0.4, 0.5, 0.6, 0.7, 0.8, 0.9, 1.0 equiv., respectively) in ethanol-water ($V : V = 9 : 1$) solution with an excitation at 322 nm. Insert: Fluorescence intensity ratio at two peaks ($F_{520 \text{ nm}}/F_{511 \text{ nm}}$) versus the concentration of Zn^{2+} over the range 0 to 50 μM .

in compound **1** was deprotonated upon binding with Zn^{2+} , which strengthened the electron-accepting ability of the hydrazone nitrogen atom from the coumarin unit, and the intramolecular charge transfer (ICT) process from the coumarin unit to the hydrazone nitrogen atom enhanced [54–56] (Scheme 2). As a result, the fluorescence emission was red-shifted upon addition of Zn^{2+} . Moreover, the ratio of fluorescence emission intensities at 520 nm and 511 nm ($F_{520 \text{ nm}}/F_{511 \text{ nm}}$) increased from 0.890 to 1.102 with Zn^{2+} equivalence up to 0.5, and almost no changes were observed in the ratio with further addition of Zn^{2+} (Fig. 2), indicating that a 2 : 1 complex was formed between compound **1** and Zn^{2+} . Interestingly, when we chose the absorption band of complex **1**- Zn^{2+} at 342 nm or 474 nm as an excitation wavelength, the fluorescence emission spectra of **1** in the presence of 5.0 equiv. of Zn^{2+} were similar with that upon excitation at 322 nm, but a few differences in fluorescence emission intensity were observed (Fig. S3). Therefore, this compound **1** could be utilized as a ratiometric fluorescent probe

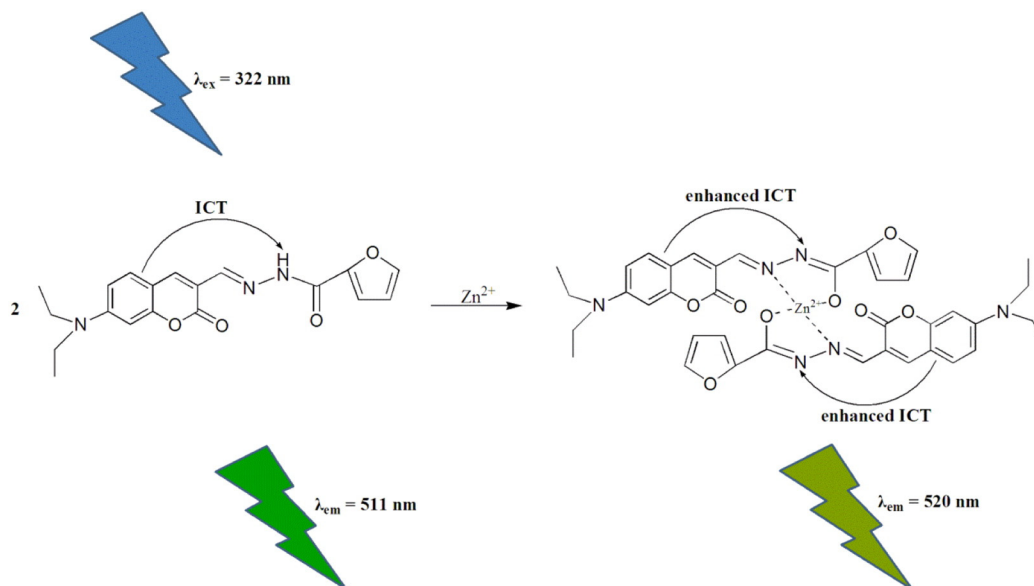
for the quantitative detection of Zn^{2+} in ethanol-water system with excited at 322 nm.

3.4. The Effect of Reaction Time on the Fluorescence Response of Compound **1** to Zn^{2+}

We explored the effect of reaction time on the fluorescence response of compound **1** to Zn^{2+} to determine if **1** could be used as a Zn^{2+} ratiometric fluorescent probe for real-time detection. For this purpose, the ratios of fluorescence emission intensities at 520 nm and 511 nm ($F_{520 \text{ nm}}/F_{511 \text{ nm}}$) were recorded at different time in ethanol-water ($V : V = 9 : 1$) solution of compound **1** in the presence of 5.0 equiv. of Zn^{2+} . As depicted in Fig. S4, the ratio increased rapidly and nearly saturated within 0.5 min, and almost no further changes were obtained with more reaction time (Fig. S4), which demonstrated that the ratiometric fluorescence response of compound **1** to Zn^{2+} was so fast that **1** could be utilized as a Zn^{2+} ratiometric fluorescent probe for real-time detection.

3.5. Selectivity of Compound **1** towards Zn^{2+} over Other Metal Ions

Selectivity is an important factor that can develop a certain fluorescent probe for broad applications. The selectivity of compound **1** towards Zn^{2+} over other chemically and biologically important metal ions was then examined by adding a variety of respective metal ions to the ethanol-water ($V : V = 9 : 1$) solution of **1**. As illustrated in Fig. 3 (a), with excited at 322 nm, compound **1** in the absence of any metal ion displayed an intense emission peak centered at 511 nm, which was red-shifted to 520 nm in the presence of 5 equiv. of Zn^{2+} , and the fluorescence emission intensity at 511 nm decreased to a certain degree upon addition of 5 equiv. of Co^{2+} , Cu^{2+} , Fe^{3+} and Ni^{2+} . The reason was probably attributed to the paramagnetic properties of these four metal ions, so when they were binding with probes, the emission would be strongly quenched via a photoinduced metal to fluorophore electron or energy transfer mechanism [57–60]. However, the addition of other metal ions induced slight or no changes in the fluorescence emission spectrum of compound **1** (Fig. 3 (a)). In addition, the ratios of fluorescence emission intensities at 520 nm and 511 nm ($F_{520 \text{ nm}}/F_{511 \text{ nm}}$) were recorded in the mixtures of **1** and respective metal ions, and it showed a significant increase in the presence of Zn^{2+} (Fig. 3 (b)). From the results above, it was concluded that



Scheme 2. The proposed binding mechanism for the response of **1** to Zn^{2+} .

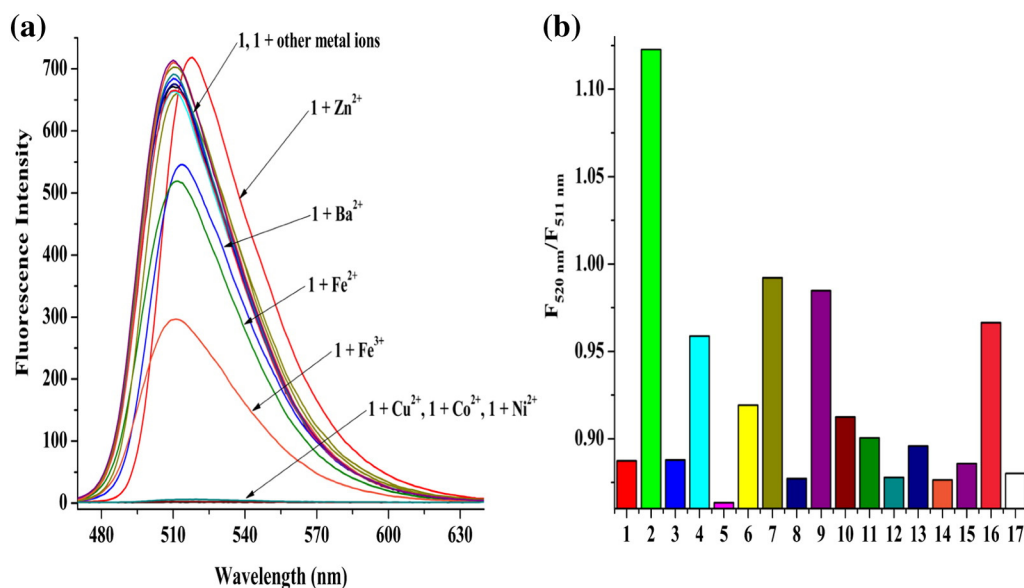


Fig. 3. (a) Fluorescence emission spectrum of **1** (50 μM) in the absence and presence of various respective metal ions (5 equiv.) in ethanol-water (V : V = 9 : 1) solution with an excitation at 322 nm. (b) Ratiometric fluorescence response profile changes ($F_{520\text{ nm}}/F_{511\text{ nm}}$) of **1** (50 μM) in the presence of various respective metal ions (5 equiv.) under the identical conditions in ethanol-water (V : V = 9 : 1) solution. ((1) **1**; (2) **1** + Zn^{2+} ; (3) **1** + Al^{3+} ; (4) **1** + Ba^{2+} ; (5) **1** + Ca^{2+} ; (6) **1** + Cd^{2+} ; (7) **1** + Co^{2+} ; (8) **1** + Cr^{3+} ; (9) **1** + Cu^{2+} ; (10) **1** + Fe^{2+} ; (11) **1** + Fe^{3+} ; (12) **1** + K^+ ; (13) **1** + Mg^{2+} ; (14) **1** + Mn^{2+} ; (15) **1** + Na^+ ; (16) **1** + Ni^{2+} ; (17) **1** + Pb^{2+}) ($\lambda_{\text{ex}} = 322\text{ nm}$, slit: 3.0/1.5 nm).

compound **1** had good selectivity towards Zn^{2+} over other common metal ions investigated with ratiometric fluorescence response.

In order to further explore the selectivity of compound **1** towards Zn^{2+} in the presence of other interfering metal ions, competition experiments were carried out by adding other respective metal ions (5 equiv.) to the ethanol-water (V : V = 9 : 1) solution of **1** with Zn^{2+} (5 equiv.) and the results were illustrated in Fig. 4. The fluorescence emission intensity at 520 nm quenched remarkably in the solution of **1** with Zn^{2+} in the presence of Co^{2+} , Cu^{2+} , Fe^{3+} and Ni^{2+} , and Al^{3+} , Cr^{3+} , Fe^{2+} also decreased the fluorescence emission intensity at 520 nm to a certain degree. However, nearly no changes were observed in the case of other metal ions tested (Fig. 4 (a)). On the other hand, the ratio of

fluorescence emission intensities at 520 nm and 511 nm ($F_{520\text{ nm}}/F_{511\text{ nm}}$) showed negligible changes upon addition of all the metal ions to the solution of **1** with Zn^{2+} except for Al^{3+} , Cr^{3+} , Cu^{2+} , Fe^{2+} and Fe^{3+} , which slightly enhanced or decreased the value of $F_{520\text{ nm}}/F_{511\text{ nm}}$. Interestingly, the addition of Cd^{2+} also caused almost no change in the ratio and had no influence on the ratiometric detection of Zn^{2+} by **1** (Fig. 4 (b)). These results suggested that the ratiometric detection had more accurate responses that could eliminate the interferences from other metal ions than intensity-based detection. Therefore, compound **1** had good selectivity towards Zn^{2+} in the presence of most coexisting metal ions, because most metal ions investigated did not interfere with the ratiometric detection of Zn^{2+} by **1**.

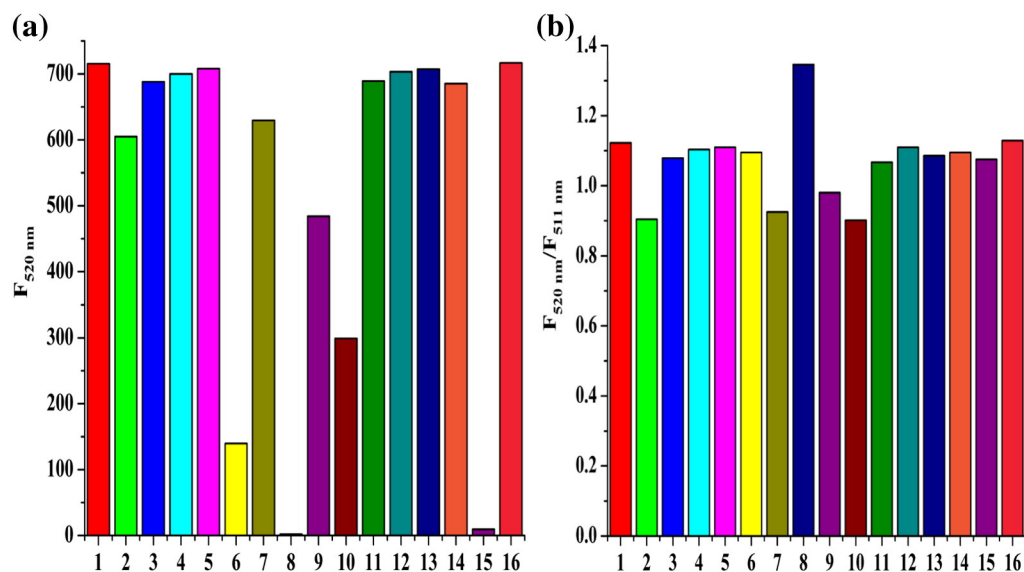


Fig. 4. (a) Fluorescence response profile changes at 520 nm of **1** (50 μM) with Zn^{2+} (5 equiv.) in the presence of other respective metal ions (5 equiv.) under the identical conditions in ethanol-water (V : V = 9 : 1) solution. (b) Ratiometric fluorescence response profile changes ($F_{520\text{ nm}}/F_{511\text{ nm}}$) of **1** (50 μM) with Zn^{2+} (5 equiv.) in the presence of other respective metal ions (5 equiv.) under the identical conditions in ethanol-water (V : V = 9 : 1) solution. ((1) Zn^{2+} ; (2) Zn^{2+} + Al^{3+} ; (3) Zn^{2+} + Ba^{2+} ; (4) Zn^{2+} + Ca^{2+} ; (5) Zn^{2+} + Cd^{2+} ; (6) Zn^{2+} + Co^{2+} ; (7) Zn^{2+} + Cr^{3+} ; (8) Zn^{2+} + Cu^{2+} ; (9) Zn^{2+} + Fe^{2+} ; (10) Zn^{2+} + Fe^{3+} ; (11) Zn^{2+} + K^+ ; (12) Zn^{2+} + Mg^{2+} ; (13) Zn^{2+} + Mn^{2+} ; (14) Zn^{2+} + Na^+ ; (15) Zn^{2+} + Ni^{2+} ; (16) Zn^{2+} + Pb^{2+}) ($\lambda_{\text{ex}} = 322\text{ nm}$, slit: 3.0/1.5 nm).

3.6. Binding Stoichiometry between Compound **1** and Zn^{2+}

A Job's plot was then explored to verify the binding stoichiometry between compound **1** and Zn^{2+} . For this purpose, the total concentration of compound **1** and Zn^{2+} was kept constant at 100 μM , and the ratio of fluorescence emission intensities at 520 nm and 511 nm ($F_{520\text{ nm}}/F_{511\text{ nm}}$) was plotted as the molar ratio of Zn^{2+} in complex **1**- Zn^{2+} . As can be seen from Fig. 5, the value of $F_{520\text{ nm}}/F_{511\text{ nm}}$ reached maximum at the molar ratio of 0.3, demonstrating a 2 : 1 binding stoichiometry between compound **1** and Zn^{2+} in ethanol-water (V : V = 9 : 1) solution, which was consistent well with the fluorescence titration experiments. On a basis of 2 : 1 binding stoichiometry, the binding constant (K) of compound **1** with Zn^{2+} was estimated from fluorescence titration experiments by the Benesi-Hildebrand equation (1) and the result was found to be $1.58 \times 10^8\text{ M}^{-0.5}$ (Fig. S5), which was within the range 10^3 – 10^9 of those reported Zn^{2+} fluorescent probes [61–64].

The limit of detection (LOD) is one of the most important parameters in designing fluorescent probes for metal ions detection. For many practical purposes, it is very significant to detect analytes at low concentrations. On a basis of this fact, we calculated the LOD value of compound **1** for sensing Zn^{2+} from fluorescence titration experiments and the result was illustrated in Fig. S6. A linear relationship between the fluorescence emission intensities ratio $F_{520\text{ nm}}/F_{511\text{ nm}}$ and the concentration of Zn^{2+} was obtained in the range of 0–0.45 μM ($R^2 = 0.9864$). Based on the results above, the LOD value was calculated to be $1.13 \times 10^{-7}\text{ M}$ (Fig. S6), which was comparable to those previously reported Zn^{2+} fluorescent probes [65–67] and was lower than the amount of labile Zn^{2+} in human bodies [68]. Thus, this compound **1** showed high sensitivity for Zn^{2+} and could be applied for sensing Zn^{2+} in environmental and biological systems.

3.7. The Effect of pH on the Fluorescence Response of Compound **1** to Zn^{2+}

In order to investigate if our synthesized compound **1** could be applied for detecting and recognizing Zn^{2+} under physiological conditions, the effect of pH on the fluorescence response of **1** to Zn^{2+} was further conducted by recording the fluorescence emission intensity at 520 nm ($F_{520\text{ nm}}$) and the ratio of fluorescence emission intensities at 520 nm and 511 nm ($F_{520\text{ nm}}/F_{511\text{ nm}}$) as a function of pH in ethanol-water (V : V = 9 : 1) solution of **1** in the absence and presence of Zn^{2+} (5.0 equiv.). As can be seen from Fig. S7, in the case of compound **1** in the absence and presence of Zn^{2+} , the values of $F_{520\text{ nm}}$ both

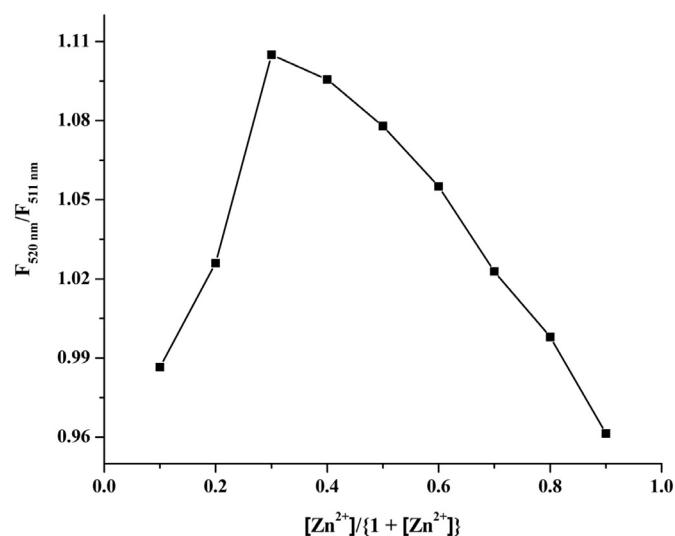


Fig. 5. Job's plot for determining the stoichiometry between **1** and Zn^{2+} in ethanol-water (V : V = 9 : 1) solution ($X_{Zn} = [Zn^{2+}]/([Zn^{2+}] + [1])$), the total concentration of **1** and Zn^{2+} was 100 μM).

reached the highest at a pH range from 6 to 7, but decreased with the pH changing from 6 to 1. Furthermore, almost no fluorescence emission at 520 nm was observed under alkaline conditions (Fig. S7 (a)). Additionally, in the pH range of 7–11, the values of $F_{520\text{ nm}}/F_{511\text{ nm}}$ of **1** with Zn^{2+} were higher than that of **1** alone. However, when pH decreased or increased, a sharp decrease was observed in compound **1** in the presence of Zn^{2+} , and the values of $F_{520\text{ nm}}/F_{511\text{ nm}}$ of **1** with Zn^{2+} were lower than that of free **1** (Fig. S7 (b)). It was mainly due to the protonation process of the Schiff-base nitrogen atom in compound **1** under acidic conditions, which weakened its binding with Zn^{2+} . Moreover, the hydrolysis process of Zn^{2+} was observed under alkaline conditions, which reduced the concentration of complex **1**- Zn^{2+} in the system. From the results above, it was concluded that our synthesized compound **1** could be utilized as a Zn^{2+} ratiometric fluorescent probe in neutral environments and applied for detecting and recognizing Zn^{2+} under physiological conditions.

3.8. Reversibility and Regeneration of Compound **1** for Sensing Zn^{2+}

In order to broaden the applications of compound **1** in environmental and biological systems, we examined if this compound **1** had good reversibility and regeneration for sensing Zn^{2+} in ethanol-water system. For this purpose, EDTANa₂, which was a good chelating agent with metal ions, was added to a mixture of **1** and Zn^{2+} (5 equiv.) in ethanol-water (V : V = 9 : 1) solution. As illustrated in Fig. 6, a red-shift was observed in fluorescence emission spectrum of **1** upon addition of Zn^{2+} , which was blue-shifted again with introduction of 5 equiv. of EDTANa₂, and the obtained fluorescence emission spectrum was almost the same as that of free **1** (Fig. 6). These results demonstrated that this compound **1** had good reversibility and regeneration for sensing Zn^{2+} in ethanol-water system, so that it could be applied for detecting Zn^{2+} in environmental and biological systems.

3.9. ¹H NMR Experiments

Finally, ¹H NMR spectra of compound **1** in the absence and presence of 1.0 equiv. of Zn^{2+} were carried out to further explore the binding mechanism for the response of **1** to Zn^{2+} , and spectral changes of compound **1** upon addition of $Zn(NO_3)_2 \cdot 6H_2O$ in CDCl₃ were depicted in Fig. 7. When Zn^{2+} was added to the solution of **1**, the proton signal of the imino group (—NH—) was shifted downfield significantly from δ

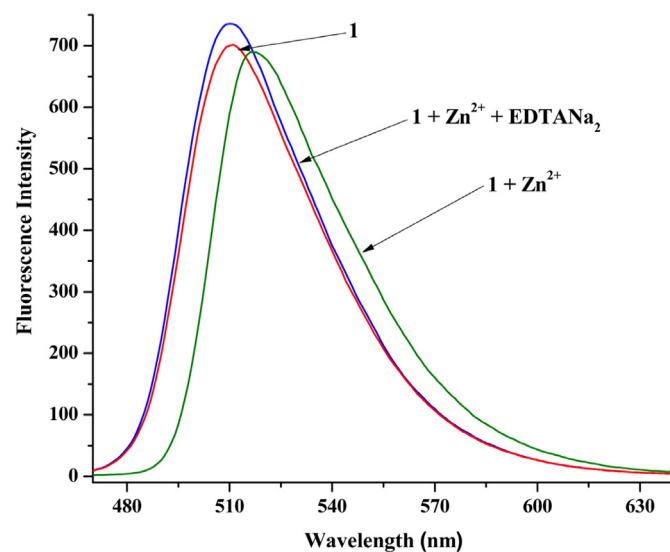


Fig. 6. Change in fluorescence emission spectrum of **1** (50 μM) with Zn^{2+} (5 equiv.) upon addition of EDTANa₂ (5 equiv.) in ethanol-water (V : V = 9 : 1) solution with an excitation at 322 nm.

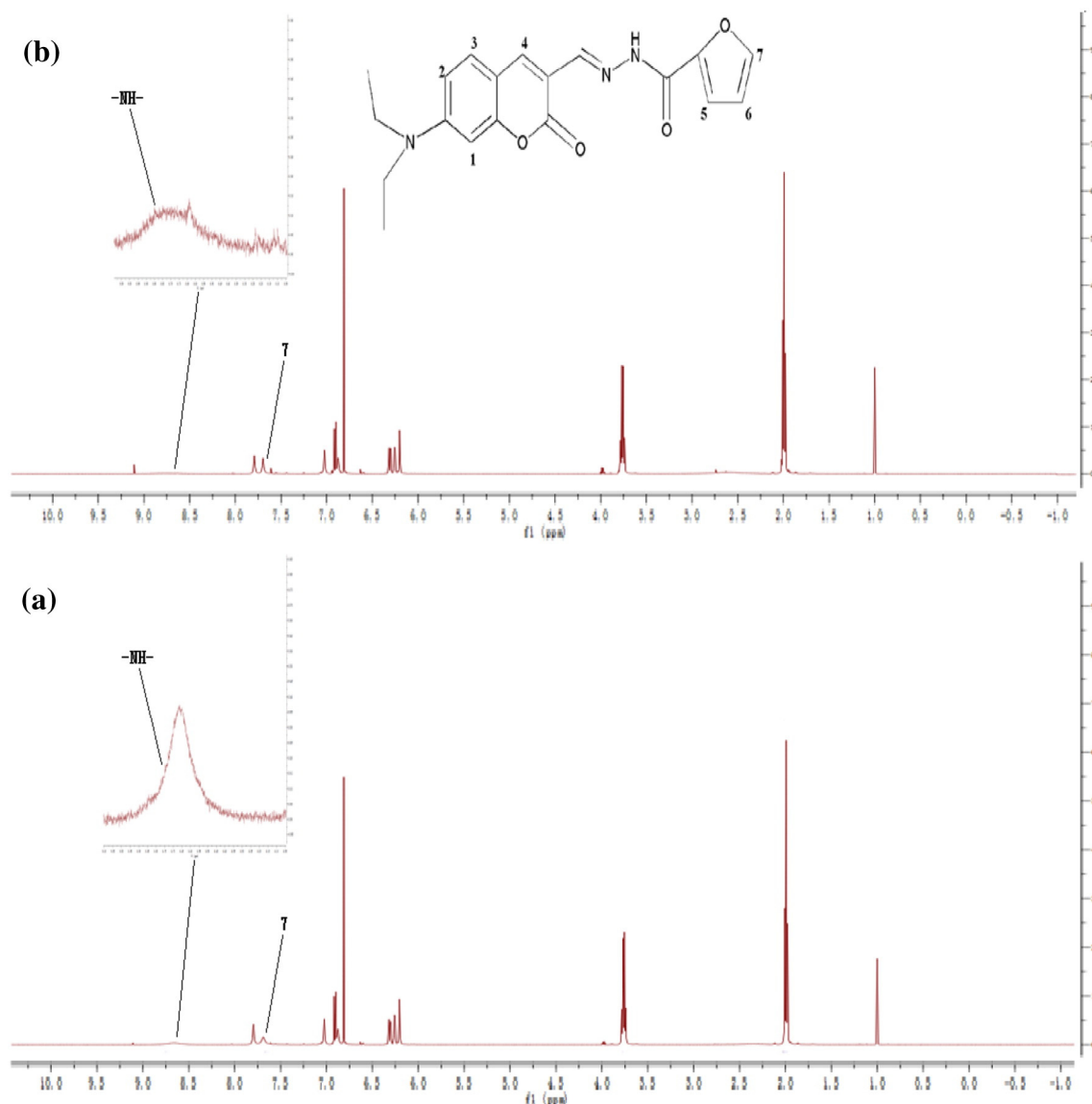


Fig. 7. ^1H NMR spectra of **1** upon addition of Zn^{2+} in CDCl_3 (a) **1**; (b) **1** and Zn^{2+} (1.0 equiv.).

8.663 ppm to δ 8.747 ppm with a decrease in its integral area. Simultaneously, the signal of the seventh proton H_7 of the furan moiety was also shifted downfield slightly from δ 7.689 ppm to δ 7.697 ppm. Nevertheless, nearly no changes in chemical shifts of other protons in compound **1** were obtained in the presence of Zn^{2+} (Fig. 7), suggesting that the oxygen atom of the carbonyl group from hydrazone and the Schiff-base nitrogen atom in compound **1** took part in the coordination and formed a 2 : 1 complex with Zn^{2+} (Scheme 2), which corresponded well with the fluorescence titration experiments and Job's plot analysis.

4. Conclusion

In conclusion, a novel coumarin-derived compound **1** bearing the furan moiety was designed, synthesized and characterized by ^1H NMR spectrum and ESI-MS spectrum. This compound **1** showed ratiometric fluorescence response to Zn^{2+} with a gradual decrease at 511 nm and a gradual enhancement at 520 nm in ethanol-water ($V : V = 9 : 1$) solution. Moreover, compound **1** had good selectivity and high sensitivity towards Zn^{2+} over other common metal ions, for the limit of detection (LOD) of **1** for sensing Zn^{2+} could reach 1.13×10^{-7} M, and most metal ions investigated did not interfere with the ratiometric detection of

Zn^{2+} by **1**. In addition, the ratiometric fluorescence response of compound **1** to Zn^{2+} was so fast, and 2 : 1 binding stoichiometry between **1** and Zn^{2+} was determined by fluorescence titration experiments, Job's plot analysis and ^1H NMR experiments. As a result, this compound **1** could be utilized as a ratiometric fluorescent probe for detecting and monitoring Zn^{2+} in ethanol-water system for real-time detection and applied for sensing Zn^{2+} in environmental and biological systems. Furthermore, the applications of novel sensors for detecting biologically and environmentally important metal ions in real samples are ongoing in our laboratory.

Acknowledgments

This work is supported by the National Natural Science Foundation of China (81171337). Gansu NSF (1308RJZ115).

Appendix A. Supplementary data

Supplementary data to this article can be found online at <http://dx.doi.org/10.1016/j.saa.2016.11.034>.

References

- [1] C. Andreini, L. Banci, I. Bertini, A. Rosato, Zinc through the three domains of life, *J. Proteome Res.* 5 (2006) 3173–3178.
- [2] K.A. McCall, C. Huang, Carol, Function and mechanism of zinc metalloenzymes, *J. Nutr.* 130 (2000) 1437–1446.
- [3] S. Enthaler, X.F. Wu, M. Weidauer, E. Irran, P. Dohler, Exploring the coordination chemistry of 2-picolinic acid to zinc and application of the complexes in catalytic oxidation chemistry, *Inorg. Chem. Commun.* 46 (2014) 320–323.
- [4] Y.C. Han, C.C. Fu, J.F. Kuang, J.Y. Chen, W.J. Lu, Two banana fruit ripening-related C₂H₂ zinc finger proteins are transcriptional repressors of ethylene biosynthetic genes, *Postharvest Biol. Technol.* 116 (2016) 8–15.
- [5] H. Yang, Z.Y. Huang, J. Li, Y. Hu, MT-like proteins: potential bio-indicators of *Chlorella vulgaris* for zinc contamination in water environment, *Ecol. Indic.* 45 (2014) 103–109.
- [6] D.K. Khajuria, C. Disha, R. Vasireddi, R. Razdan, D.R. Mahapatra, Risedronate/zinc-hydroxyapatite based nanomedicine for osteoporosis, *Mater. Sci. Eng. C* 63 (2016) 78–87.
- [7] L. Chen, W.H. Yung, Zinc modulates GABAergic neurotransmission in rat globus pallidus, *Neurosci. Lett.* 409 (2006) 163–167.
- [8] E. Mrkalic, A. Zianna, G. Psomas, M. Gdaniec, A. Czapiak, E. Coutouli-Argyropoulou, M. Lalia-Kantouri, Synthesis, characterization, thermal and DNA-binding properties of new zinc complexes with 2-hydroxyphenones, *J. Inorg. Biochem.* 134 (2014) 66–75.
- [9] D. Ferro, N. Franchi, V. Mangano, R. Bakiu, M. Cammarata, N. Parrinello, G. Santovito, L. Ballarin, Characterization and metal-induced gene transcription of a new copper-zinc superoxide dismutases in the solitary ascidian *Ciona intestinalis*, *Aquat. Toxicol.* 140–141 (2013) 369–379.
- [10] N. Pourhassanali, S. Roshan-Milani, F. Kheradmand, M. Motazakker, M. Bagheri, E. Saboori, Zinc attenuates ethanol-induced Sertoli cell toxicity and apoptosis through caspase-3 mediated pathways, *Reprod. Toxicol.* 61 (2016) 97–103.
- [11] G. Huang, L.Q. Mo, J.L. Cai, X. Cao, Y. Peng, Y.A. Guo, S.J. Wei, Environmentally friendly and efficient catalysis of cyclohexane oxidation by iron meso-tetrakis(pentafluorophenyl)porphyrin immobilized on zinc oxide, *Appl. Catal. B Environ.* 162 (2015) 364–371.
- [12] M. Guzman-Rivero, A. Verduguez-Orellana, M. Cordova, L. Maldonado, M. Medina, E. Sejas, B. Akesson, Effect of zinc on immune functions in patients with pulmonary tuberculosis, *Biomed. Prev. Nutr.* 4 (2014) 245–250.
- [13] J. Appgar, Zinc and reproduction: an update, *J. Nutr. Biochem.* 3 (1992) 266–278.
- [14] H. Kaya, F. Aydin, M. Gurkan, S. Yilmaz, M. Ates, V. Demir, Z. Arslan, A comparative toxicity study between small and large size zinc oxide nanoparticles in tilapia (*Oreochromis niloticus*): organ pathologies, osmoregulatory responses and immunological parameters, *Chemosphere* 144 (2016) 571–582.
- [15] M. Valko, H. Morris, M.T. Cronin, Metals, toxicity and oxidative stress, *Curr. Med. Chem.* 12 (2005) 1161–1208.
- [16] A.M. Hessel, M. Merx, Genetically-encoded FRET-based sensors for monitoring Zn²⁺ in living cells, *Metalomics* 7 (2015) 258–266.
- [17] N.L. Bjorklund, V.M. Sadagoparamanujam, G. Tagliatalata, Selective, quantitative measurement of releasable synaptic zinc in human autopsy hippocampal brain tissue from Alzheimer's disease patients, *J. Neurosci. Meth.* 203 (2012) 146–151.
- [18] J.H. Viles, Metal ions and amyloid fiber formation in neurodegenerative diseases. Copper, zinc and iron in Alzheimer's, Parkinson's and prion diseases, *Coord. Chem. Rev.* 256 (2012) 2271–2284.
- [19] M. Seven, S.Y. Basaran, M. Cengiz, S. Unal, A. Yuksel, Deficiency of selenium and zinc as a causative factor for idiopathic intractable epilepsy, *Epilepsy Res.* 104 (2013) 35–39.
- [20] B.G. Jang, S.J. Won, J.H. Kim, B.Y. Choi, M.W. Lee, M. Sohn, H.K. Song, S.W. Suh, EAAC1 gene deletion alters zinc homeostasis and enhances cortical neuronal injury after transient cerebral ischemia in mice, *J. Trace Elem. Med. Biol.* 26 (2012) 85–88.
- [21] E.J. McAllum, B.R. Roberts, J.L. Hickey, T.N. Dang, A. Grubman, P.S. Donnelly, J.R. Liddell, A.R. White, P.J. Crouch, Zn^{II}(atm) is protective in amyotrophic lateral sclerosis model mice via a copper delivery mechanism, *Neurobiol. Dis.* 81 (2015) 20–24.
- [22] M. Karamali, Z. Heidarzadeh, S.M. Seifati, M. Samimi, Z. Tabassi, M. Hajjajafari, Z. Asemi, A. Esmaillzadeh, Zinc supplementation and the effects on metabolic status in gestational diabetes: a randomized, double-blind, placebo-controlled trial, *J. Diabetes Complicat.* 29 (2015) 1314–1319.
- [23] H.P.S. Sachdev, N.K. Mittal, H.S. Yadav, 50 – A controlled trial on the utility of oral zinc supplementation in chronic diarrhea in infancy, *Malnutr. Chro. Diet-Assoc. Infant. Diarrh.* 429–432 (1990).
- [24] T. Jiang, X.H. Xiong, S.X. Wang, Y.L. Luo, Q. Fei, A.M. Yu, Z.Q. Zhu, Direct mass spectrometric analysis of zinc and cadmium in water by microwave plasma torch coupled with a linear ion trap mass spectrometer, *Int. J. Mass Spectrom.* 399–400 (2016) 33–39.
- [25] S. Kumari, S. Joshi, T.C. Cordova-Sintjago, D.D. Pant, R. Sakhuja, Highly sensitive fluorescent imidazolium-based sensors for nanomolar detection of explosive picric acid in aqueous medium, *Sensor. Actuat. B Chem.* 229 (2016) 599–608.
- [26] S.D. Wang, X.L. Fei, J. Guo, Q.B. Yang, Y.X. Li, Y. Song, A novel reaction-based colorimetric and ratiometric fluorescent sensor for cyanide anion with a large emission shift and high selectivity, *Talanta* 148 (2016) 229–236.
- [27] H.L. Nie, W. Yang, M.Q. Yang, J. Jing, X.L. Zhang, Highly specific and ratiometric fluorescent probe for ozone assay in indoor air and living cells, *Dyes Pigments* 127 (2016) 67–72.
- [28] S. Mukherjee, P. Mal, H. Stoekli-Evans, Turn-on and reversible luminescent sensor for selective recognition of Al³⁺ using naphthol hydrazone, *J. Lumin.* 172 (2016) 124–130.
- [29] K. Chantalakana, N. Choengchan, P. Yingyud, P. Thongyoo, A highly selective 'turn-on' fluorescent sensor for Zn²⁺ based on fluorescein conjugates, *Tetrahedron Lett.* 57 (2016) 1146–1149.
- [30] J.H. Hu, J.B. Li, J. Qi, Y. Sun, Acylhydrazone based fluorescent chemosensor for zinc in aqueous solution with high selectivity and sensitivity, *Sensor. Actuat. B Chem.* 208 (2015) 581–587.
- [31] Z.P. Dong, Y.P. Guo, X. Tian, J.T. Ma, Quinoline group based fluorescent sensor for detecting zinc ions in aqueous media and its logic gate behavior, *J. Lumin.* 134 (2013) 635–639.
- [32] W.G. Wang, R. Li, T.W. Song, C.J. Zhang, Y. Zhao, Study on the fluorescent chemosensors based on a series of bis-Schiff bases for the detection of zinc(II), *Spectrochim. Acta Part A Mol. Biomol. Spectrosc.* 164 (2016) 133–138.
- [33] Z.L. Gong, B.X. Zhao, W.Y. Liu, H.S. Lv, A new highly selective "turn on" fluorescent sensor for zinc ion based on a pyrazoline derivative, *J. Photochem. Photobiol. A Chem.* 218 (2011) 6–10.
- [34] C.J. Gao, X.J. Jin, X.H. Yan, P. An, Y. Zhang, L.L. Liu, H. Tian, W.S. Liu, X.J. Yao, Y. Tang, A small molecular fluorescent sensor for highly selectivity of zinc ion, *Sensors Actuat. B Chem.* 176 (2013) 775–781.
- [35] H. Ming, R. Naidu, B. Sarkar, D.T. Lamb, Y.J. Liu, M. Megharaj, D. Sparks, Competitive sorption of cadmium and zinc in contrasting soils, *Geoderma* 268 (2016) 60–68.
- [36] J. Cherif, N. Derbel, M. Nakkach, H.V. Bergmann, F. Jemal, Z.B. Lakhdar, Spectroscopic studies of photosynthetic responses of tomato plants to the interaction of zinc and cadmium toxicity, *J. Photochem. Photobiol. B Biol.* 111 (2012) 9–16.
- [37] M. Ozdemir, A selective fluorescent 'turn-on' sensor for recognition of Zn²⁺ in aqueous media, *Spectrochim. Acta Part A Mol. Biomol. Spectrosc.* 161 (2016) 115–121.
- [38] C.C. Woodrooffe, S.J. Lippard, A novel two-fluorophore approach to ratiometric sensing of Zn²⁺, *J. Am. Chem. Soc.* 125 (2003) 11458–11459.
- [39] D.D. Li, Y.N. Shi, X.H. Tian, M.M. Wang, B. Huang, F. Li, S.L. Li, H.P. Zhou, J.Y. Wu, Y.P. Tian, Fluorescent probes with dual-mode for rapid detection of SO₂ derivatives in living cells: ratiometric and two-photon fluorescent sensors, *Sensors Actuat. B Chem.* 233 (2016) 1–6.
- [40] A.M. Hessel, P. Chabosseau, M.H. Bakker, W. Engelen, G.A. Rutter, K.M. Taylor, M. Merx, eZinCh-2: a versatile, genetically encoded FRET sensor for cytosolic and intracellular Zn²⁺ imaging, *ACS Chem. Biol.* 10 (2015) 2126–2134.
- [41] J. Geng, Y. Liu, J.H. Li, G. Yin, W. Huang, R.Y. Wang, Y.W. Quan, A ratiometric fluorescent probe for ferric ion based on a 2,2'-bithiazole derivative and its biological applications, *Sensors Actuat. B Chem.* 222 (2016) 612–617.
- [42] Y. Zhang, X.F. Guo, X.J. Tian, A.D. Liu, L.H. Jia, Carboxamidoquinoline-coumarin derivative: a ratiometric fluorescent sensor for Cu(II) in a dual fluorophore hybrid, *Sensor. Actuat. B Chem.* 218 (2015) 37–41.
- [43] Y.H. Zhang, Y.Y. Yan, S.Y. Chen, Z.N. Gao, H. Xu, 'Naked-eye' quinoline-based 'reactive' sensor for recognition of Hg²⁺ ion in aqueous solution, *Bioorg. Med. Chem. Lett.* 24 (2014) 5373–5376.
- [44] N. Singh, N. Kaur, R.C. Mulrooney, J.F. Callan, A ratiometric fluorescent probe for magnesium employing excited state intramolecular proton transfer, *Tetrahedron Lett.* 49 (2008) 6690–6692.
- [45] E.N. Kaya, F. Yuksel, G.A. Ozpinar, M. Bulut, M. Durmus, 7-Oxy-3-(3,4,5-trimethoxyphenyl)coumarin substituted phthalonitrile derivatives as fluorescent sensors for detection of Fe³⁺ ions: experimental and theoretical study, *Sensors Actuat. B Chem.* 194 (2014) 377–388.
- [46] H.X. Xu, X.Q. Wang, C.L. Zhang, Y.P. Wu, Z.P. Liu, Coumarin-hydrazone based high selective fluorescence sensor for copper(II) detection in aqueous solution, *Inorg. Chem. Commun.* 34 (2013) 8–11.
- [47] J.J. Ma, R.L. Sheng, J.S. Wu, W.M. Liu, H.Y. Zhang, A new coumarin-derived fluorescent sensor with red-emission for Zn²⁺ in aqueous solution, *Sensors Actuat. B Chem.* 197 (2014) 364–369.
- [48] S.T. Wang, G. Ge, S.F. Guo, Y. Ma, F.C. Qiu, X.Y. Jian, R.F. Chen, Chinese Journal of Pharmaceutical 22 (1991) 396–397.
- [49] J.C. Qin, Z.Y. Yang, Design of a novel coumarin-based multifunctional fluorescent probe for Zn²⁺/Cu²⁺/S²⁻ in aqueous solution, *Mater. Sci. Eng. C* 57 (2015) 265–271.
- [50] Y.K. Jang, U.C. Nam, H.L. Kwon, I.H. Hwang, C. Kim, A selective colorimetric and fluorescent chemosensor based-on naphthol for detection of Al³⁺ and Cu²⁺, *Dyes Pigments* 99 (2013) 6–13.
- [51] T.J. Jia, W. Cao, X.J. Zheng, L.P. Jin, A turn-on chemosensor based on naphthol-triazole for Al(III) and its application in bioimaging, *Tetrahedron Lett.* 54 (2013) 3471–3474.
- [52] G.L. Long, J.D. Winefordner, Limit of detection a closer look at the IUPAC definition, *Anal. Chem.* 55 (1983) 712A–724A.
- [53] C.R. Lohani, J.M. Kim, S.Y. Chung, J. Yoon, K.H. Lee, Colorimetric and fluorescent sensing of pyrophosphate in 100% aqueous solution by a system comprised of rhodamine B compound and Al³⁺ complex, *Analyst* 135 (2010) 2079–2084.
- [54] Z.F. Li, Y.X. Sun, H. Li, J.K. Ren, C.F. Si, X. Lv, J.S. Yu, H. Wang, F. Shi, Y.Y. Hao, Efficient blue fluorescent electroluminescence based on a *tert*-butylated 9,9'-bianthracene derivative with a twisted intramolecular charge-transfer excited state, *Synth. Met.* 217 (2016) 102–108.
- [55] T. Kuwabara, X.Y. Tao, H.C. Guo, M. Katsumata, H. Kurokawa, Monocationic ionophores capable of ion-responsive intramolecular charge transfer absorption variation, *Tetrahedron* 72 (2016) 1069–1075.
- [56] S. Phukan, M. Saha, A.K. Pal, A.C. Bhasikuttan, S. Mitra, Intramolecular charge transfer in coumarin based donor-acceptor systems: formation of a new product through planar intermediate, *J. Photochem. Photobiol. A Chem.* 303–304 (2015) 67–79.
- [57] L. Wannasen, E. Swatsitang, Magnetic properties dependence on Fe²⁺/Fe³⁺ and oxygen vacancies in SrTi_{0.95}Fe_{0.05}O₃ nanocrystalline prepared by hydrothermal method, *Microelectron. Eng.* 146 (2015) 92–98.
- [58] T. Fichtner, G. Kreiner, S. Chadov, G.H. Fecher, W. Schnelle, A. Hoser, C. Felser, Magnetic and transport properties in the Heusler series Ni_{2-x}Mn_{1+x}Sn affected by chemical disorder, *Intermetallics* 57 (2015) 101–112.
- [59] Y.Z. Voloshin, A.Y. Lebedev, V.V. Novikov, A.V. Dolganov, A.V. Vologzhanina, E.G. Lebed, A.A. Pavlov, Z.A. Starikova, M.I. Buzin, Y.N. Bubnov, Template synthesis, X-

- ray structure, spectral and redox properties of the paramagnetic alkylboron-capped cobalt(II) clathrochelates and their diamagnetic iron(II)-containing analogs, *Inorg. Chim. Acta* 399 (2013) 67–78.
- [60] A.M. Elshahawy, M.H. Mahmoud, S.A. Makhlof, H.H. Hamdeh, Role of Cu^{2+} substitution on the structural and magnetic properties of Ni-ferrite nanoparticles synthesized by the microwave-combustion method, *Ceram. Int.* 41 (2015) 11264–11271.
- [61] K. Wechakorn, K. Suksen, P. Piyachaturawat, P. Kongsaree, Rhodamine-based fluorescent and colorimetric sensor for zinc and its application in bioimaging, *Sensor. Actuat. B Chem.* 228 (2016) 270–277.
- [62] X.J. Tian, X.F. Guo, F.S. Yu, L.H. Jia, An oxalamidoquinoline-based fluorescent sensor for selective detection of Zn^{2+} in solution and living cells and its logic gate behavior, *Sensor. Actuat. B Chem.* 232 (2016) 181–187.
- [63] R. Borthakur, U. Thapa, M. Asthana, S. Mitra, K. Ismail, R.A. Lal, A new dihydrazone based “turn on” fluorescent sensor for Zn(II) ion in aqueous medium, *J. Photochem. Photobiol. A Chem.* 301 (2015) 6–13.
- [64] X.H. Tian, X.F. Guo, L.H. Jia, R. Yang, G.Z. Cao, C.Y. Liu, A fluorescent sensor based on bicarboxamidoquinoline for highly selective relay recognition of Zn^{2+} and citrate with ratiometric response, *Sensor. Actuat. B Chem.* 221 (2015) 923–929.
- [65] A.B. Pradhan, S.K. Mandal, S. Banerjee, A. Mukherjee, S. Das, A.R.K. Bukhsh, A. Saha, A highly selective fluorescent sensor for zinc ion based on quinoline platform with potential applications for cell imaging studies, *Polyhedron* 94 (2015) 75–82.
- [66] S.S. Mati, S. Chall, S. Konar, S. Rakshit, S.C. Bhattacharya, Pyrimidine-based fluorescent zinc sensor: photo-physical characteristics, quantum chemical interpretation and application in real samples, *Sensor. Actuat. B Chem.* 201 (2014) 204–212.
- [67] J.C. Qin, L. Fan, Z.Y. Yang, A small-molecule and resumable two-photon fluorescent probe for Zn^{2+} based on a coumarin Schiff-base, *Sensor. Actuat. B Chem.* 228 (2016) 156–161.
- [68] S. Tajik, M.A. Taher, A new sorbent of modified MWCNTs for column preconcentration of ultra trace amounts of zinc in biological and water samples, *Desalination* 278 (2011) 57–64.